Flow-induced resonance shift in sonic slit array metamaterials

J. Christensen[1,2,*] and M. Willatzen[2]
[1]*IQFR - CSIC Serrano 119, 28006 Madrid, Spain*
[2]*Mads Clausen Institute, University of Southern Denmark, Alsion 2, DK-6400 Sønderborg, Denmark*
(Received 28 December 2011; revised manuscript received 22 February 2012; published 21 March 2012)

A modal analysis of flow-acoustic wave propagation through slit array metamaterials is presented. It is demonstrated that the transmission-coefficient change versus flow speed is a sensitive function of frequency. Our results further confirm that transmission resonance positions and resonance widths change significantly with the flow speed. As a reverse application, the present metamaterial slit structures allow for flow tuning of slit cavity modes, design of surface bound states such as superlens applications where a broad frequency operation interval is sought. Finally, it is shown rather surprisingly that the flow-acoustic coupling is almost independent of the angle of incidence.

DOI: 10.1103/PhysRevB.85.094304 PACS number(s): 42.25.Bs, 67.80.de

I. INTRODUCTION

About a decade ago it was demonstrated that light propagation through subwavelength perforated metallic films shows the extraordinary optical transmission (EOT) due to surface plasmonic effects.[1] For one individual subwavelength hole in a screen of zero thickness, the transmission would rapidly drop off at a rate $(r/\lambda)^4$ above cutoff, but in the particular periodic configuration by Ebbesen, it was shown that also the light impinging on the metal between the holes is transmitted through the film. Although there has been a great deal of debate and controversy behind the mechanism of EOT, it is now widely accepted and supported by a variety of experimental observations and theoretical predictions that a resonant excitation of surface plasmon polaritons (SPPs) on and through the structure gives rise to the observation of enhanced transmission.[2,3]

Stimulated by the above results for optical wave propagation through holey films, several recent contributions have been presented for the case of sound waves impinging on screens containing subwavelength perforations. This phenomenon of enhanced sound transmission in small holes has been demonstrated for isolated apertures,[4] slit and hole arrays[5–8] such as the bull's eye structure,[9,10] and compound arrangements.[11,12] Other related phenomena associated to sound waves in holey structures are the resonant transmission in structured plates without openings[13,14] and the design of geometry induced surface modes.[15–17]

Many facets of acoustic metamaterial exist for the control of sound waves. One example is the design of anisotropic acoustic parameters, which is an important aspect of transformation acoustics.[18–20] We believe by introducing a fluid flow as a design strategy for tuning acoustic metamaterial properties will broaden the range of fascinating new phenomena. Likewise, in the field of optical metamaterials, we have witnessed a large variety of tuning-recipes relying on modifying dielectric environments, applying mechanical strain, biasing graphene-plasmonic building blocks, or introducing optofluidic coupling.[21–24] We investigate flow-acoustic transmission through a periodic slit array and, in particular, the possibility to tune in frequency transmission to resonance where a high sensitivity toward a background flow is obtained. In hindsight, we notice that the sensitivity in typical transit-time based ultrasonic flowmeters is estimated to[25–29]

$$\frac{\Delta T}{T} = 2\frac{u_0}{c_0}, \tag{1}$$

where ΔT, T, u_0, and c_0 are the difference in transit time between upstream and downstream flow situations, the transit time at zero flow, the background flow velocity, and the speed of sound, respectively.

This paper is organized as follows. For a specific slit width and slit length, the transmission coefficient is computed as a function of frequency and flow speed in cases where the acoustic waves propagate along and against the direction of flow speed. It is demonstrated that transmission resonances change location and widths as the flow speed changes. By varying the slit length for a fixed slit width, and vice versa, optimized sensitivities at specific frequencies against flow can be obtained. Since the acoustic cavity and surface mode locations depend strongly on the flow speed, the present transmission measurement setup can be used to obtain bound surface states and cavity modes for a large operation frequency interval of relevance in, e.g., superlens applications. As a corollary, our results show the rather surprising result that flow-acoustic coupling is almost insensitive to the acoustic wave direction of incidence.

II. THEORETICAL FORMALISM

Consider a low-amplitude acoustic field in a steady-moving inviscid fluid. We assume that the fluid is moving at uniform speed u_0 along the z axis in the semi-infinite regions before and after the slit as well as in the slab (in the latter, however, with a higher uniform flow value) such that no turbulent motions are regarded. The speed of sound c_0 remains unaltered by the background flow relative to the medium, but the propagating acoustic wave is said to be convected downstream by the mean flow. We explain this by the following expressions for the conservation of mass and momentum:

$$\begin{aligned} \frac{D\rho}{Dt} + \rho_0 \nabla \cdot \boldsymbol{v} &= 0, \\ \rho_0 \frac{D\boldsymbol{v}}{Dt} + \nabla p &= 0, \end{aligned} \tag{2}$$

where the total rate of change $\frac{D}{Dt} = \frac{\partial}{\partial t} + u_0 \frac{\partial}{\partial z}$ accounts for the time rate of a moving frame and u_0 is the flow speed along the z axis. ρ_0 is the mass density of the background fluid whereas $p, \boldsymbol{v}$ and ρ refer to the acoustic quantities of pressure, velocity, and density, respectively. Together with the isentropic relationship we can combine these two equations so as to obtain the convective (along z) wave equation:

$$\frac{D^2 p}{Dt^2} = \left(\frac{\partial}{\partial t} + u_0 \frac{\partial}{\partial z}\right)^2 p = c_0^2 \nabla^2 p. \tag{3}$$

The influence on sound propagation in the presence of a moving background can be expressed by the wave number parallel to the traveling wave:

$$\beta = \sqrt{k^2 - k_x^2} = \sqrt{\frac{(\omega - \beta u_0)^2}{c_0^2} - k_x^2}, \tag{4}$$

discarding variations along the homogeneous y direction. Equation (4) tells us that the free-space wave number, ordinarily written as $k(u_0 = 0) = \omega/c_0$, now is altered by the Mach number $M = u_0/c_0$ along β such that $k(u_0 \neq 0) = \omega/c_0 - \beta M$. When solving the actual flow acoustical problem in the slit array metamaterial, we will present β in isolated form as compared to Eq. (4), and calculate the implications of the flow on the resonant modes. The sketch in Fig. 1 shows a perfect rigid slab into which slits of width a are cut periodically with lattice constant Λ. Although this slab has a finite thickness h we illustrate the structure with a broken section, because in the theoretical formalism we will treat the upper and lower interfaces as two separate semispaces. Afterwards in the transmission study, we introduce a phase delay through the slab controlled by h that connects the two interfaces. Following a modal expansion procedure, we express the pressure and the normal component of sound velocity undergoing continuity across the first interface, by their incident and reflected plane

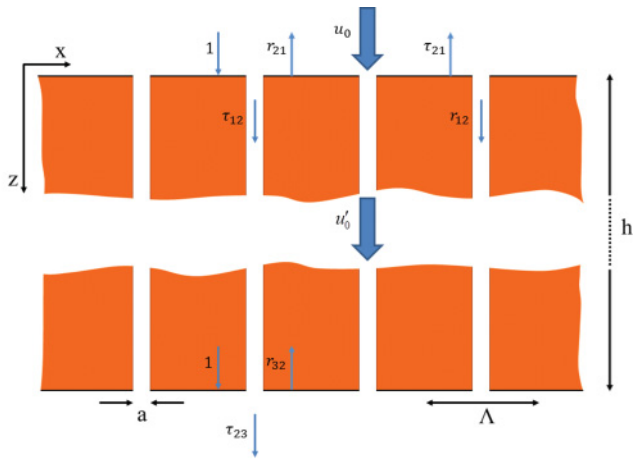

FIG. 1. (Color online) Sketch of a perfect rigid slit array metamaterial under study. The structure contains periodic cuts along the x axis that are separated by Λ. The width of the slits is a, whereas the thickness is h. At the upper interface, we express the scattering coefficients τ_{12}, τ_{21}, r_{21}, r_{12} such as τ_{23}, r_{32} at the lower interface. The moving background flow with a uniform speed u_0 outside and u_0' inside the metamaterial.

waves:

$$\begin{aligned} |p^{\mathrm{I}}\rangle &= Z_+^0 |k_x^0\rangle e^{-i\beta_+^0 z} + \sum_{n=-\infty}^{\infty} r_{21} Z_-^n |k_x^n\rangle e^{i\beta_-^n z}, \\ |v_z^{\mathrm{I}}\rangle &= -|k_x^0\rangle e^{-i\beta_+^0 z} + \sum_{n=-\infty}^{\infty} r_{21} |k_x^n\rangle e^{i\beta_-^n z}, \end{aligned} \tag{5}$$

such as a one-way wave traveling with the fundamental cavity mode through the slits:

$$\begin{aligned} |p^{\mathrm{II}}\rangle &= \tau_{12} Z_+' |0\rangle e^{-i\beta_+' z}, \\ |v_z^{\mathrm{II}}\rangle &= -\tau_{12} |0\rangle e^{-i\beta_+' z}. \end{aligned} \tag{6}$$

Equation (6) is the unambiguous evidence that the first interface separating the wave impinging and penetrating side has been treated as a halfspace with no back-reflecting wave components inside the slits. The wave number is written as $\beta_\pm^n = k_0 \frac{g^n \mp M}{1 - M^2}$, where $g^n = \sqrt{1 - (\frac{k_x^n}{k_0})^2 (1 - M^2)}$ with $k_0 = 2\pi/\lambda$ and $k_x^n = k_x^0 + \frac{2\pi}{\Lambda} n$. Note that normal specular radiation yields $g^0 = 1$, which is independent of flow. However, the impedance of the perforated structure is modulated by the moving media: $Z_\pm^n = k_0/\beta_\pm^n - M$.

In a similar fashion, we express the variables for waves traveling inside the slit cavity, carried by its fundamental waveguide mode $|0\rangle$. We write the wave number for propagating waves as $\beta_\pm' = k_0 \frac{g' \mp M'}{1 - M'^2}$, where $g' = 1$ and $Z_\pm' = k_0/\beta_\pm' - M'$. In order to preserve continuity of mass across the interface of constricted width, we write the Mach number for the slits as $M' = M\Lambda/a$. Next, we impose steadiness of the pressure and the normal velocity component containing the mass flow while, respectively, projecting them over the fundamental mode inside the slit aperture and into a set of plane waves. This is expressed by two equations of continuity:

$$\begin{aligned} Z_+^0 G_0 + \sum_{n=-\infty}^{\infty} r_{21} Z_-^n G^n &= \tau_{12} Z_+' \\ -\delta_{0n} + r_{21} &= -\tau_{12} G^n, \end{aligned} \tag{7}$$

where $G^n = \sqrt{\frac{a}{\Lambda}}\,\mathrm{sinc}(k_x^n a/2)$. Conclusively, we can solve for the scattering (Fresnel) coefficients τ_{12} and r_{21} at the first interface:

$$\begin{aligned} \tau_{12} &= \frac{2G^0(1 - M)}{\sum_{n=-\infty}^{\infty} Z_-^n |G^n|^2 + Z_+'}, \\ r_{21} &= \delta_{0n} - \tau_{12} G^n, \end{aligned} \tag{8}$$

which are nothing but semi-analytical expressions for the transmission and reflection coefficients at a perforated half space under the influence of flow. A likewise procedure is applied for the wave emerging at the lower interface of the structure in Fig. 1. We decompose the problem into a bidirectional wave motion inside the slits and plane waves that are scattered into free space when emerging the slit array. Thus we have for the cavity region:

$$\begin{aligned} |p^{\mathrm{II}}\rangle &= Z_+' |0\rangle e^{-i\beta_+' z} + r_{32} Z_-' |0\rangle e^{i\beta_-' z}, \\ |v_z^{\mathrm{II}}\rangle &= -|0\rangle e^{-i\beta_+' z} + r_{32} |0\rangle e^{i\beta_-' z}, \end{aligned} \tag{9}$$

where the variables are similarly described as from Eq. (6), now, however, with different scattering coefficients. When the waves finally emerge into free space, the field is diffracted (with the order n) and weighted by its corresponding transmission coefficient τ_{23}:

$$|p^{\mathrm{III}}\rangle = \sum_{n=-\infty}^{\infty} \tau_{23} Z_+^n \left|k_x^n\right\rangle e^{-i\beta_+^n z},$$
$$\left|v_z^{\mathrm{III}}\right\rangle = -\sum_{n=-\infty}^{\infty} \tau_{23} \left|k_x^n\right\rangle e^{-i\beta_+^n z}. \tag{10}$$

Also at the lower interface continuity has to be maintained for the pressure p across the slits while being projected over cavity modes $\langle 0|$ and naturally also for v_z across the unit cell but over plane waves $\langle k_x^{n'}|$:

$$Z'_+ + r_{32} Z'_- = \sum_{n=-\infty}^{\infty} \tau_{23} Z_+^n G^n.$$
$$(1 - r_{32}) G^n = \tau_{23}. \tag{11}$$

To this end, we can solve the scattering coefficients governing the lower interface which read

$$\tau_{23} = \frac{2G^n(1 - M')}{\sum_{n=-\infty}^{\infty} Z_+^n |G^n|^2 + Z'_-},$$
$$r_{32} = \frac{\sum_{n=-\infty}^{\infty} Z_+^n |G^n|^2 - Z'_+}{\sum_{n=-\infty}^{\infty} Z_+^n |G^n|^2 + Z'_-}. \tag{12}$$

In order to express the overall transmission coefficient t_n after multiple scattering events through the slitted metamaterial (see Fig. 1), we gather the scattering coefficients τ_{12}, r_{21} [see Eq. (8)] and τ_{23}, r_{32} [see Eq. (12)] from the separated half spaces by introducing a finite slab thickness h. When writing t_n comprising the sequential round trips through the slit array, special attention is required to account for the flow direction during the phase build-up. Hence we can write t_n comprising down- and upstream scattering as

$$t_n = \tau_{12}\tau_{23} e^{i\beta'_+ h} + \tau_{12} r_{32} r_{12} \tau_{23} e^{i\beta'_+ h} e^{i(\beta'_+ + \beta'_-)h}$$
$$+ \tau_{12} r_{32}^2 r_{12}^2 \tau_{23} e^{i\beta'_+ h} e^{2i(\beta'_+ + \beta'_-)h} \cdots = \frac{\tau_{12}\tau_{23} e^{i\beta'_+ h}}{1 - r_{32} r_{12} e^{i(\beta'_+ + \beta'_-)h}}. \tag{13}$$

This expression will serve as an important tool in order to study the influence of fluid flow through a rigid periodic slit array. Although we have treated the slit array at their separating faces, an entire scattering problem of this periodic structure of finite thickness is formulated, given the formulas derived for the Fresnel coeffcients [see Eqs. (8) and (12)]. In the next section, we will present numerous simulations for acoustic waves funnelled through these subwavelength structures and study how the moving background can help in tuning the transparent windows of full transmission based on resonances.

III. ANALYSIS

To investigate the coupling of a moving media with sound waves while studying the tunability of a slit array under the influence of flow, we chose a great variety of geometrical

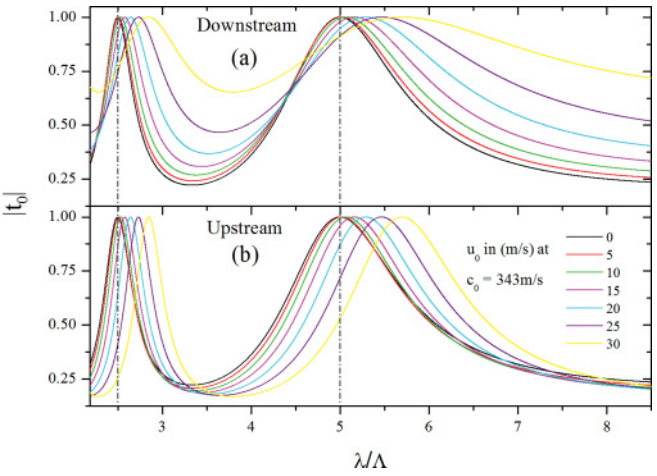

FIG. 2. (Color online) Simulated modulus of the zero-order transmission coefficient $|t_0|$ vs normalized wavelength (λ/Λ) for a slit array metamaterial with the geometrical parameters chosen to be $a = 0.25\Lambda$ and $h = 2.5\Lambda$. The two vertical dash-dotted lines mark the spectral location for the two lowest ($m = 1,2$) Fabry-Perot resonances when the medium is at rest, $u_0 = 0$. (a) Transmission spectra for sound propagating downstream or (b) upstream in air. We have chosen the background flow to be in the range $u_0 = 0$–30 m/s. The incident sound plane wave is impinging at the normal direction.

parameters for the structure under study. This allows us to elaborate the acoustic response for different values of u_0 in a large range of angular and spectral values. We have carried out a seminumerical implementation of Eq. (13) comprising the scattering coefficients described in the latter section and initially chosen a metamaterial of fixed geometries. In Fig. 2, we render $|t_0|$ at normal incidence for a structure containing slit width $a = 0.25\Lambda$ and thickness $h = 2.5\Lambda$. Note that all geometrical parameters including the spectrum of wavelength under study are normalized to the lattice constant Λ. By doing so one can scale the structure at will in order to study the flow acoustic resonances both in the kHz or MHz regimes. We have chosen the background medium to be air ($\rho = 1.28$ kg/m^3, $c_0 = 343$ m/s, for all simulations) which is steadily and uniformly moving ($\nabla \cdot \mathbf{u_0} = 0$) through the structure. Figure 2 plots transmittance spectra in the range of the two lowest order Fabry-Perot resonances that are found at $\lambda_m = 2h/m$ with $m = 1,2,\ldots$.[4] For both panels, we see resonance-induced transmittance peaks indicated with vertical dash-dotted lines in a medium at rest, $u_0 = 0$. When the flow sets in we predict a resonance shift toward lower frequencies, irrespective of the flow direction relative to the direction of impinging sound. This shift is clearly growing with increasing flow speed and shows a second-order polynomial dependence. If sound is propagating upstream as calculated in Fig. 2(b), the transmittance peaks remain narrow but shifted to lower frequencies as mentioned earlier. In the case of downstream wave propagation, the resonance shift is accompanied by a broadening of the transmission peaks, which is clearly seen in Fig. 2(a). This observation not only predicts a significant influence of flow on the slit cavity induced transparent acoustic spectrum, in actual fact, it also consolidates the nonreciprocal nature in flow-acoustic problems characterized by resonance broadening. We wish to emphasize that the Doppler effect

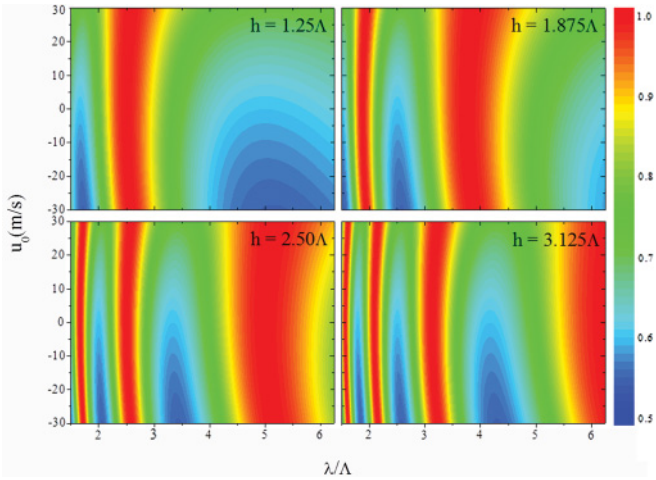

FIG. 3. (Color online) $|t_0|$ contour versus normalized wavelength (λ/Λ) and u_0 at normal incidence. For all four simulated examples, we fix the slit width to $a = 0.5\Lambda$, but as illustrated in the panels we vary the slab thickness between $h = 1.25\Lambda$, 1.875Λ, 2.5Λ, and 3.125Λ.

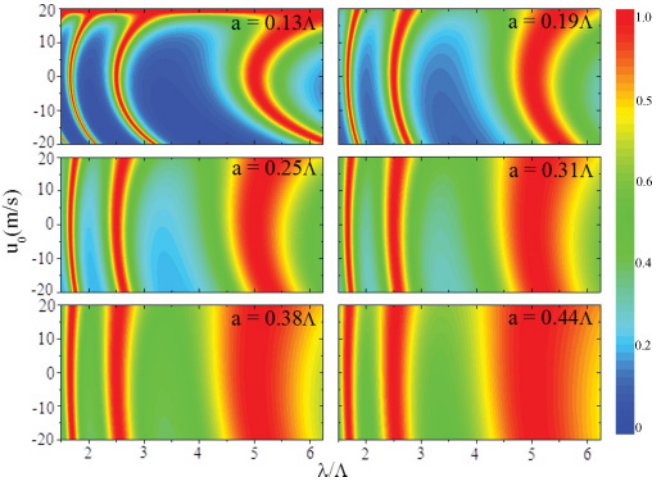

FIG. 4. (Color online) $|t_0|$ contour vs normalized wavelength (λ/Λ) and u_0 at normal incidence. For the six simulated examples we fix the thickness to $h = 2.5\Lambda$, but as illustrated in the panels, we calculate various slit widths ranging from $a = 0.13\Lambda$ to 0.44Λ.

does not play a role here since the frequency is unaffected by the presence of flow and we neglect the relative motion between the acoustic source and receiver. The sole effect of the background flow is to modify the local wave speed through modulation of the local wavelength.

In the following, we shall undertake a parametrical study to obtain further insight into the flow-borne phenomena. For this matter, we fix the slit width a but increase the "channel length" for different values of the thickness h. Initially, we can prove the stationary case ($u_0 = 0$) for all chosen geometries ($h = 1.25\Lambda$, 1.875Λ, 2.5Λ, and 3.125Λ) as illustrated in Fig. 3. As expected, the larger h is the larger is the set of lambda-half resonances that fits inside the slits which results in an increased number of transmission peaks induced by Fabry-Perot resonances. Akin to the results from Fig. 2, we also predict, as plotted in Fig. 3, that the flow is forcing resonance shifts toward lower frequencies that sustain for Fabry-Perot resonances of higher order $\lambda_m = 2h/m$ with $m = 1,2,3,\ldots$. This, in fact, has the consequence that the flow-induced transmission shift prevails for a broad range of frequencies but of discrete nature. The widths of the transmission peaks, seen for all chosen thicknesses h, depend on the sign of the velocity u_0 of the moving media. Yet it seems that higher-order modes supported in thick structures, e.g., $h = 3.125\Lambda$, are symmetric in their peak width irrespective of the sign of the flow and only the frequency shift prevails.

If we instead vary the width of the slit a, strong changes occur for the Mach number M' inside the slit to fulfill mass conservation. A small width would cause large values of u_0' in order to preserve the same mass flowing into and through the slitted metamaterial. We fix the slab thickness to $h = 2.5\Lambda$ but calculate six examples of different widths ranging from $a = 0.13\Lambda$ to 0.44Λ as seen in Fig. 4. For relatively large yet subwavelength $\lambda > \Lambda > a$ widths of $a \geqslant 0.31\Lambda$, Fig. 4 plots $|t_0|$ contours where the coupling strength seems rather moderate as the resonant peaks in these three examples ($a = 0.31\Lambda$, 0.38Λ, and 0.44Λ) change slightly only.

Narrowing the widths down corresponding to $a = 0.13\Lambda$, 0.19Λ, and 0.25Λ shows a strong sensitivity and eventually a large offset in the spectral locations of transmission resonances relative to the medium at rest ($u_0 = 0$). In view of the extraordinary transmission of sound through subwavelength apertures,[4] we can report that the apertures under the influence of flow appear to be smaller compared to the wavelength. As the flow leads to full transmission at larger wavelengths as opposed to the situation with the background medium at rest, the factor ka at resonance is forced to decrease and enhanced transmission is obtained. In particular, when $a = 0.13\Lambda$, we see a broad spectrum of full transmission when $u_0 \approx 20$ m/s and a region appears for which all discrete Fabry-Perot modes merge into a wide band. However, due to the large flow speed inside the slits in this case, we will not here extend these discussions further. Large Mach numbers inside an orifice of narrow cross section could put the assumption of uniform flow, as we tacitly assumed throughout this work, into question.

It is known that Fabry-Perot resonances are dispersionless flat modes comprising transparent windows for both propagating and evanescent waves.[30] Figure 5(a) is a plot of the band diagram in a spectrum showing the first two cavity resonances. Here, we initially compute the stationary case for a slit array with $a = 0.13\Lambda$ and $h = 3.75\Lambda$ but the central and the right panel of Fig. 5 render dispersion relations for $u_0 = 15$ and -15 m/s, respectively. One could expect that the flow-acoustic coupling strength decreases when the angle of incident sound $[\theta = \sin^{-1}(k_x/k_0)]$ deviates from the flow direction. It is, however, not the case. The flow remains unchanged directed along the z axis and as the Fabry-Perot modes remain undispersed as a function of k_x, refer to Fig. 5(a), we see as shown in Figs. 5(b) and 5(c) that the characteristics of frequency shift and band broadening prevail. In the frequency spectrum of interest, we now see that a third resonance-induced transmission peak emerges due to a shift. Sound waves propagating with flow [see Fig. 5(b)] are giving rise to band broadening for all angles of incident sound

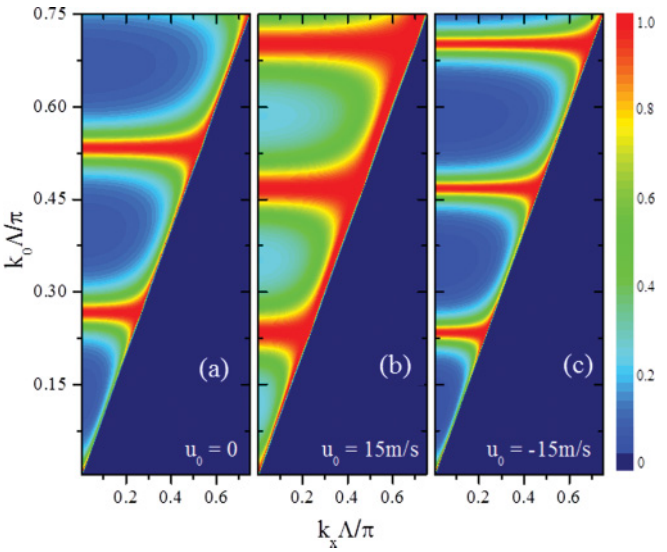

FIG. 5. (Color online) Dispersion relations for a structure with the geometrical parameters: $a = 0.13\Lambda$ and $h = 3.75\Lambda$ rendering $|t_0|$ versus parallel momentum ($k_x\Lambda/\pi$) and free-space wave number ($k_0\Lambda/\pi$). For the three panels, we calculate the bands in the range $k_0 > k_x$. Left panel, as illustrated corresponds to $u_0 = 0$, whereas the remaining to panels predict the behavior of $|t_0(k_0,k_x,u_0)|$ for $u_0 = 15$ and -15 m/s.

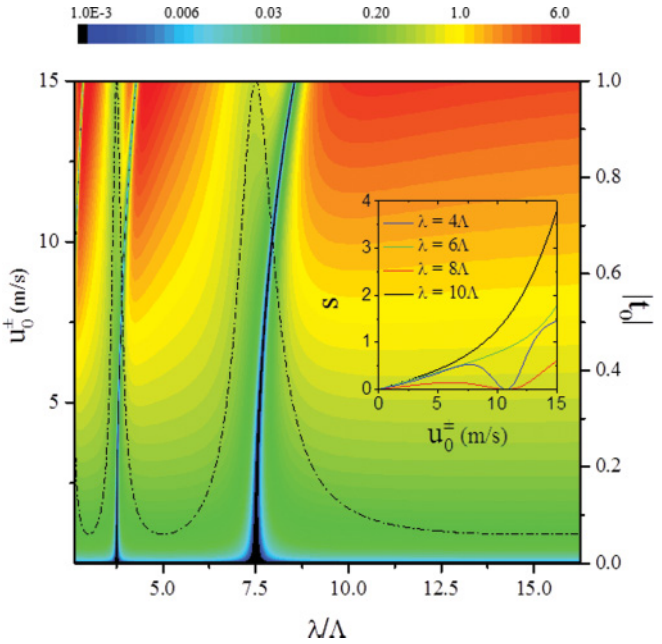

FIG. 6. (Color online) Computation of flow sensitivity S vs frequency for a metamaterial slit structure with parameters $a = 0.13\Lambda$ and $h = 3.75\Lambda$. Dash-dotted line plots $|t_0|$ for $u_0 = 0$. Inset: S for specific chosen values of the ratio λ/Λ.

whereas sharp and narrow modes are sustained against the flow [see Fig. 5(c)]. In previous works, it was pointed out that transmission resonances in slitted metamaterials stem from the excitation of acoustic guided waves that hybridize strongly with Fabry-Perot resonances associated with slit cavities. These surface modes have been studied on a separate basis in connection with the tunability and guidance of acoustic waves along structured surfaces.[15,16] Concerning this matter it is clear that slit arrays belong to the same family of patterned guides. Now with the new property to tune those cavity modes to lower frequencies by the influence of flow, the possibility to design bound states of increased surface confinement, $k_x \gg k_0$, becomes possible. Recently, it has also been suggested that perforated acoustic metamaterials can act as superlenses capable to recover deep subwavelength details of acoustic images.[30] The limitation, however, is that those systems again are based on resonances and strictly induced by geometrical means. It is therefore a possible tuning strategy to use a moving background medium to control and enhance the operating efficiency of a superlens metamaterial. With a background flow of $u_0 = 15$ m/s as shown in Fig. 5(b), operation at different center-frequencies is possible (shifted Fabry-Perot resonances, also for $k_x > k_0$, however, not shown) where, in addition, resonances are broader compared to resonances for a background medium at rest. This means that off-resonance issues can be tackled easier due to full transmission bands of larger width.

IV. FLOW SENSITIVITY

We next discuss the present principle's sensitivity against a background flow. In Fig. 6, the relative difference in transmission amplitude in cases with flow along and against the direction of impinging sound waves, defined as the sensitivity S, is plotted

$$S = \frac{T(u_0^+) - T(u_0^-)}{T_0}, \tag{14}$$

where $T(u_0^+)$, $T(u_0^-)$, and T_0 are the transmission coefficient with flow along the impinging sound wave direction, the transmission coefficient with flow against the impinging sound wave direction, and the transmission coefficient at zero flow, respectively. Obviously, at resonance peaks, the sensitivity is zero but away from resonance the sensitivity increases strongly. Indeed, there are large regions of frequencies where the sensitivity is substantially larger than 1 if the flow velocity is above 5 m/s. At these frequencies, the sensitivity of the present method largely surpasses the frequency-independent sensitivity of a transit-time flow measurement being $\Delta T/T = 2u_0/c$. It is evident from the insert of Fig. 6 that a large sensitivity is obtained at a large ratio λ/Λ, e.g., when $\lambda/\Lambda = 10$, the sensitivity is high and almost linear for flow values in the range 0–10 m/s, while at flow values above 10 m/s, it increases in a superlinear fashion. Indeed, in the smaller flow range 0–10 m/s, the S vs u_0 ratio is equal to about 0.1 s/m, i.e., much higher than the same ratio $2/c \approx 0.006$ s/m for the transit-time method, refer to Eq. (1). Importantly, the transmission at zero flow is still reasonably high (about 0.1, see dash-dotted line in Fig. 6) when $\lambda/\Lambda = 10$ so signal-to-noise ratios are acceptable.

V. CONCLUSION

Flow-acoustic resonance phenomena in slit array metamaterial structures are examined. It is demonstrated that acoustic transmission in a slit structure reveals resonance positions

and resonance widths that change significantly with flow. Indeed, the possibility to tune frequency and slit dimensions makes it possible to precisely determine flow speed from transmission experiments. It is rather surprisingly shown that the flow-acoustic coupling is almost insensitive to the acoustic wave angle of incidence. The present slit array configuration also provides tuning of acoustic cavity and surface bound modes by a forced and controlled background flow with potential applications in superlenses where a large operation frequency interval is sought.

ACKNOWLEDGMENTS

J.C. gratefully acknowledges financial support from The Danish Council for Independent Research (Natural Sciences) under contract Metacoustics2011 10-093234.

*johan.christensen@gmail.com

[1] T. W. Ebbesen, H. J. Lezec, H. F. Ghaemi, T. Thio, and P. A. Wolff, Nature (London) **391**, 667 (1998).
[2] F. J. Garcia de Abajo, Rev. Mod. Phys. **79**, 1267 (2007).
[3] F. J. Garcia-Vidal, L. Martin-Moreno, T. W. Ebbesen, and L. Kuipers, Rev. Mod. Phys. **82**, 729 (2010).
[4] J. Christensen, L. Martin-Moreno, and F. J. Garcia-Vidal, Phys. Rev. Lett. **101**, 014301 (2008).
[5] B. Hou, J. Mei, M. Ke, W. Wen, Z. Liu, J. Shi, and P. Sheng, Phys. Rev. B **76**, 054303 (2007).
[6] H. Estrada, P. Candelas, A. Uris, F. Belmar, F. J. García de Abajo, and F. Meseguer, Phys. Rev. Lett. **101**, 084302 (2008).
[7] R. Hao, H. Jia, Y. Ye, F. Liu, C. Qiu, M. Ke, and Z. Liu, Europhys. Lett. **92**, 24006 (2010).
[8] X. Wang, Appl. Phys. Lett. **96**, 134104 (2010).
[9] J. Christensen, A. I. Fernandez-Dominguez, F. de Leon-Perez, L. Martin-Moreno, and F. J. Garcia-Vidal, Nat. Phys. **3**, 851 (2007).
[10] J. Mei, B. Hou, M. Ke, S. Peng, H. Jia, Z. Liu, J. Shi, W. Wen, and P. Sheng, Appl. Phys. Lett. **92**, 124106 (2008).
[11] Z. Liu and G. Jin, J. Phys.: Condens. Matter **21**, 445401 (2009).
[12] H. Estrada, V. Gomez-Lozano, A. Uris, P. Candelas, F. Belmar, and F. Meseguer, J. Phys.: Condens. Matter **23**, 135401 (2011).
[13] Z. He, H. Jia, C. Qiu, S. Peng, X. Mei, F. Cai, P. Peng, M. Ke, and Z. Liu, Phys. Rev. Lett. **105**, 074301 (2010).
[14] R. Hao, C. Qiu, Y. Hu, K. Tang, and Z. Liu, Phys. Lett. A **375**, 4081 (2011).
[15] J. Christensen, L. Martin-Moreno, and F. J. Garcia-Vidal, Phys. Rev. B **81**, 174104 (2010).
[16] Z. He, H. Jia, C. Qiu, Y. Ye, R. Hao, M. Ke, and Z. Liu, Phys. Rev. B **83**, 132101 (2011).
[17] J. Christensen, L. Martin-Moreno, and F. J. Garcia-Vidal, Appl. Phys. Lett. **96**, 233505 (2010).
[18] S. A. Cummer, M. Rahm, and D. Schurig, New J. Phys. **10**, 115025 (2008).
[19] D. Torrent and J. Sanchez-Dehesa, New J. Phys. **10**, 023004 (2008).
[20] J. Li, L. Fok, X. Yin, G. Bartal, and X. Zhang, Nat. Mater. **8**, 931 (2009).
[21] M. Pryce, K. Aydin, Y. A. Kelaita, R. M. Briggs, and H. A. Atwater, Nano Lett. **8**, 4222 (2010).
[22] A. Vakil and N. Engheta, Science **332**, 1291 (2011).
[23] S. Thongrattanasiri, F. H. L. Koppens, and F. J. García de Abajo, Phys. Rev. Lett. **108**, 047401 (2012).
[24] Y. Yang, A. Q. Liu, L. K. Chin, X. M. Zhang, D. P. Tsai, C. L. Lin, C. Lu, G. P. Wang, and N. I. Zheludev, Nat. Commun. **3**, 651 (2012).
[25] L. C. Lynnworth, in *Ultrasonic Flowmeters*, edited by W. P. Mason and R. N. Thurston, Physical Acoustics, Vol. 14 (Academic, New York, 1979), p. 407.
[26] J. C. Wendoloski, J. Acoust. Soc. Am. **110**, 724 (2001).
[27] M. Willatzen, J. Acoust. Soc. Am. **109**, 102 (2001).
[28] M. Willatzen, J. Sound Vib. **247**, 719 (2001).
[29] M. Willatzen and H. Kamath, Flow Meas. Instr. **19**, 79 (2008).
[30] J. Zhu, J. Christensen, J. Jung, L. Martin-Moreno, X. Yin, L. Fok, X. Zhang, and F. J. Garcia-Vidal, Nat. Phys. **7**, 52 (2011).